

## R-eriodictyol and S-eriodictyol exhibited comparable effect against H<sub>2</sub>O<sub>2</sub>-induced oxidative stress in EA.hy926 cells

Haizhen Li, Chao Li, Tao Shen, Lijuan Zhao, Dongmei Ren\*

Key Laboratory of Chemical Biology (Ministry of Education), School of Pharmaceutical Sciences, Shandong University, Ji'nan, Shandong, China.

**Summary** Eriodictyol is a flavanone well-known for its antioxidative activity. Due to a chiral carbon atom in position C-2, eriodictyol always exist in racemic form. In order to study the antioxidant activity under H<sub>2</sub>O<sub>2</sub>-induced oxidative stress of each enantiomer, enantiomers of eriodictyol were resolved by high-performance liquid chromatography (HPLC), using a Chiral Amylose-C column as chiral stationary phase. Online coupling HPLC-circular dichroism (CD) method was used for the determination of elution order and the absolute configurations of the two eluates. The protective effects of racemic and enantiomeric eriodictyol against H<sub>2</sub>O<sub>2</sub>-induced cytotoxicity with EA.hy926 cells were tested. The results showed that the two enantiomers of eriodictyol and the corresponding racemate were equipotent, suggesting that the configuration of the C-2 chiral center does not influence the cytoprotective activity against H<sub>2</sub>O<sub>2</sub>-induced oxidative stress in EA.hy926 cells.

**Keywords:** Eriodictyol, enantiomer, cytoprotective activity, oxidative stress

### 1. Introduction

Eriodictyol, 5,7,3',4'-tetrahydroxyflavanone (Figure 1), is a chiral flavanone presented in citrus fruits and herbal products. This flavanone is well known for its beneficial health-related properties, such as antioxidant (1), antiinflammatory (2), and antimicrobial (3) activity. Recent studies have shown that eriodictyol can provide cytoprotective effect in UV-irradiated keratinocytes (4), induces long-term protection in ARPE-19 cells (5), protect neuron-like PC12 cells against H<sub>2</sub>O<sub>2</sub>-induced injury (6), prevents early retinal and plasma abnormalities in streptozotocin induced diabetic rats (7, 8).

Eriodictyol is a chiral molecule with an asymmetric center at position C-2 and can occur in two enantiomeric form, R-eriodictyol and S-eriodictyol (Figure 1). It has long been established that stereochemistry is one of the important determinant of the biological, pharmacological, and toxicological properties of many nutrients (e.g. D-glucose, L-ascorbic acid) (9) and drugs (e.g. thalidomide) (10). Thiocetic acid, a naturally occurring antioxidant, played

protective role in central nervous system injury related to oxidative stress, and only (+)-thiocetic acid showed pronounced effect both in H<sub>2</sub>O<sub>2</sub> induced cell injury or *in vivo* experiment, while (–)-thiocetic acid was inactive (11). Naringenin, which is structurally similar with eriodictyol, showed stereospecific anti-inflammatory potential *in vitro* (12). This suggested that enantiomers of flavanone might have different behaviors in pharmacological action and metabolic process (13). It is necessary to consider the stereochemistry of flavanone when studying the biological effects. However, most of published results on the biological activities of flavanone *in vitro* are available for the racemate, little is known about the influence of the stereochemical configuration of flavanone on their biological activity due to the lack of readily available pure flavanone enantiomers.

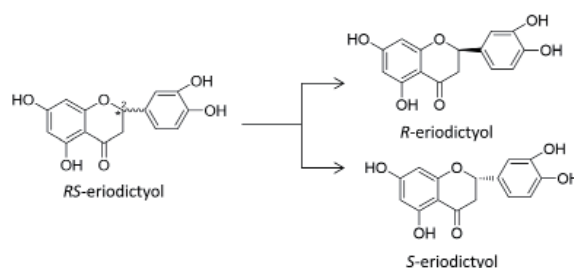


Figure 1. Structures of RS-, R- and S-eriodictyol.

\*Address correspondence to:

Dr. Dongmei Ren, School of Pharmaceutical Sciences, Shandong University, 44 Wenhuxi Road, Jinan 250012, China.

E-mail: random@sdu.edu.cn

For the separation of enantiomers of eriodictyol, a couple of methods have been previously reported, such as capillary electrophoresis (14), micellar electrokinetic chromatography (15), and chiral HPLC (16).

In our previous papers, we also described the resolution of enantiomers of some flavanones by chromatography on a chiral phase, and we reported the absolute configuration determination by CD spectra (17). However, no bioactivity study was carried out using pure enantiomers of eriodictyol. As a continuation of our research on small molecule antioxidants, this study was designed to investigate the effects of the stereochemical configuration of eriodictyol on its cytoprotective effects against oxidative stress. We have first prepared the pure enantiomeric forms of eriodictyol by chiral phase HPLC, assigned the absolute configuration by the online coupling HPLC-CD method. Furthermore, the cytoprotective abilities of *R*- and *S*-eriodictyol were tested against H<sub>2</sub>O<sub>2</sub>-induced EA.hy926 cell injury.

## 2. Materials and Methods

### 2.1. Chemicals and reagents

Racemic eriodictyol was isolated from *Dracocephalum rupestre* by the procedure of ethanol extraction, polyamide column separation and recrystallization (18). The purity was proved to be above 98% by HPLC analysis. The structure identification was carried out by <sup>1</sup>H and <sup>13</sup>C nuclear magnetic resonance (NMR). *R*- and *S*-eriodictyol were purified by chiral HPLC from racemic eriodictyol, the purities were confirmed to be above 96% by chiral HPLC-UV/CD analysis. HPLC-grade *n*-hexane and 2-propanol were from Spectrum Chemical MFG Corp. (Gardena, CA, USA). 3-(4,5-Dimethylthiazol-2-yl)-2,5-diphenyl-2H-tetrazolium bromide (MTT) was purchased from Solarbio Science & Technology Co. Ltd. (Beijing, China). 2',7'-Dichlorofluorescein diacetate (DCFH-DA) and 4',6-diamidino-2-phenylindole (DAPI) was from Sigma-aldrich (Saint Louis, MO, USA). Annexin V-FITC apoptosis detection kit was purchased from Bestbio (Shanghai, China).

### 2.2. Chromatographic system and conditions

The HPLC-UV was performed on Agilent 1260 HPLC system, equipped with quaternary pump, diode array detector and an autosampler (Agilent, Palo Alto, LA, USA). The HPLC-CD was performed on a JASCO LC-Net II/ADC HPLC system, equipped with PU-2089 plus pump, CD-2095 plus CD detector and a 7125 Rheodyne injector with 20  $\mu$ L sample loop (Jasco, Tokyo, Japan). The column (250 mm  $\times$  4.6 mm) was amylose tris-3, 5-dimethylphenyl carbamate (Chiral Amylose-C) coated on 5  $\mu$ m silica gel. The column was obtained from YMC Co. (Kyoto, Japan). Experiments were performed at ambient temperature. All solvents were degassed in an ultrasonic bath prior to use. The flow rate was 0.5 mL/min. Once a new chromatographic condition was adopted, the column

was equilibrated for at least 1 h before injection. Sample of eriodictyol was diluted in methanol to a concentration of 0.1 mg/mL for HPLC-UV and 0.5 mg/mL for HPLC-CD. The prepared HPLC sample solutions were filtered through a nonsterile 0.45  $\mu$ m PTEE syringe filter. UV and CD detection were performed at 284 nm. The CD spectra of the enantiomers were obtained by stopped-flow scanning at each chromatographic peak by CD detector from the wavelength range of 220-420 nm. Column void volume ( $t_0$ ) was measured by injection of tri-*tert*-butylbenzene as a non-retained marker. The retention factor ( $k$ ) was calculated as  $k_1 = (t_1 - t_0)/t_0$  and  $k_2 = (t_2 - t_0)/t_0$ , where  $t_1$  and  $t_2$  are the retention times for the first and second eluting enantiomers, respectively. The separation factor ( $\alpha$ ) was calculated as  $\alpha = k_2/k_1$ . The resolution factor was evaluated according to  $R_s = 2(t_2 - t_1)/(w_1 + w_2)$ , *i.e.* the peak separation divided by the mean value of the baseline widths. Retention times ( $t$ ) were mean values of two replicate determinations.

### 2.3. Cell culture and treatment

Human endothelial-like immortalized cells (EA.hy926) were obtained from the Cell Bank of Type Culture Collection of Chinese Academy of Sciences (Shanghai, China). The cells were maintained in Dulbecco's modified Eagle's medium (DMEM) (Gibco, Grand Island, NY, USA) supplemented with 10% (v/v) fetal bovine serum (FBS) (Hyclone, Logan, UT, USA), 100 U/mL penicillin and 100 U/mL streptomycin at 37°C in a humidified incubator containing 5% CO<sub>2</sub>.

### 2.4. Measurement of cell viability

Cell viability was monitored by two kinds of method. The first method is MTT assay (19). In brief,  $1 \times 10^4$  cells per well were seeded in a 96-well plate and incubated overnight. Cells were pretreated with several concentrations of compound for 2 h before exposure to H<sub>2</sub>O<sub>2</sub> for 24 h. After addition of 20  $\mu$ L 2.0 mg/mL MTT solution, the cells were incubated at 37°C for 4 h, the plate was centrifuged and the medium was removed. For each well, 100  $\mu$ L DMSO was added and crystals were dissolved by shaking the plate at room temperature. Absorbance was measured at 570 nm by a microplate reader (Biorad, Model 680, Hercules, CA, USA). Triplicate wells were used for each sample and the experiments were repeated at least three times to get means and standard deviations.

The second method is the real time cellular analysis (RTCA) by using the xCELLigence system (ACEA Biosciences, San Diego, CA, USA), which monitors cell growth in response to treatment in real-time (20). Cells grow on top of electrodes so that the impedance varies based on the number of cells attached and the quality of cell-electrode interaction. Electrode impedance, which is displayed as Cell Index (CI), can be used to monitor cell viability, number, morphology, and cell adhesion (21). Cells (10,000/well) were seeded overnight and then treated with each chemical alone or in combination, and cell growth was monitored.

### 2.5. DAPI nuclear staining

EA.hy926 cells ( $2 \times 10^5$  cells/well) in 12-well plates were exposed to compounds for 24 h, then cells were fixed in ice-cooled acetone-methanol (1:1) mixture for 5 min, after rinsing with PBS, cells were stained with DAPI (2 mg/mL) for 15 min at room temperature. Cells were viewed and photographed under fluorescence microscopy (Olympus IX71, Olympus Co., Tokyo, Japan). Apoptotic cells were recognized based on characteristic observations including the presence of condensed, fragmented and degraded nuclei.

### 2.6. Apoptosis assays

Apoptotic rates were analyzed by flow cytometry using an annexin V-FITC/PI kit (Bestbio, Shanghai, China) according to the manufacturer's instruction. Briefly, cells were treated with compounds for 24 h, and then  $1 \times 10^6$  cells were harvested, washed twice with ice-cold PBS, and evaluated for apoptosis by double staining with annexin V-FITC and propidium iodide in binding buffer using a flow cytometer (FACSCalibur, BD Biosciences, San Jose, CA, USA).

### 2.7. Measurement of intracellular Reactive oxygen species (ROS)

ROS levels were determined using DCFH-DA as fluorescent probes (22). The cells were treated with  $H_2O_2$  for 24 h after being pretreated with or without compounds for 2 h, washed cells with PBS, then incubated cells in fresh medium containing 10  $\mu$ g/mL DCFH-DA at 37°C for 30 min. Subsequently, the cells were trypsinized and diluted with PBS to approximate  $1 \times 10^6$  cells per mL, analyzed with flow cytometry at an excitation wavelength of 488 nm and an emission wavelength of 530 nm.

### 2.8. Statistical analysis

One way analysis of variance (ANOVA) and post hoc multiple comparison Bonferroni test were used to determine the significant difference between two groups. Results are presented as the mean  $\pm$  SD.  $p < 0.05$  was considered to be significant.

## 3. Results and Discussion

### 3.1. Chiral separation of eriodictyol

The effect of mobile-phase on the separation process was examined by modifying the ratio of *n*-hexane and 2-propanol. The chromatographic parameters, capacity factor ( $k$ ), separation factor ( $\alpha$ ), and resolution factor ( $R_s$ ) for the resolved eriodictyol are given in Table 1. The table showed that eriodictyol could be resolved with good separation factors ( $\alpha$ ) and resolution factors ( $R_s$ ) on Chiral Amylose-C column by optimizing the mobile phase composition. Typical enantiomeric separations of eriodictyol on Chiral

Amylose-C column and mobile phase composition are shown in Figure 2. The optimized mobile phase consisted of 30% *n*-hexane and 70% 2-propanol, and the flow rate was 0.5 mL/min. The good resolution obtained for eriodictyol allowed us to separately collect the individual enantiomers used for the biological assays. *R*- and *S*-eriodictyol (3.0 mg each) were purified using the above-mentioned optimized HPLC condition as shown in Figure 2G.

The elution order was easily determined by the online HPLC-CD method. It has been previously reported that a negative CD signal at 280-290 nm of flavanone is related to the *S*-configuration at C-2, whereas a positive CD signal establish an *R*-configuration (14). As evidenced

**Table 1. Chromatographic results for enantiomeric resolution of eriodictyol on Chiral Amylose-C CSP**

Eluent	$k_1$	$k_2$	$R_s$	$\alpha$
2-Propanol	0.37	0.47	0.85	1.27
<i>n</i> -Hexane-2-propanol 5:95	0.37	0.47	0.91	1.27
<i>n</i> -Hexane-2-propanol 10:90	0.38	0.49	0.95	1.29
<i>n</i> -Hexane-2-propanol 15:85	0.38	0.51	1.12	1.34
<i>n</i> -Hexane-2-propanol 20:80	0.39	0.54	1.19	1.38
<i>n</i> -Hexane-2-propanol 25:75	0.42	0.58	1.28	1.38
<i>n</i> -Hexane-2-propanol 30:70	0.46	0.64	1.49	1.39

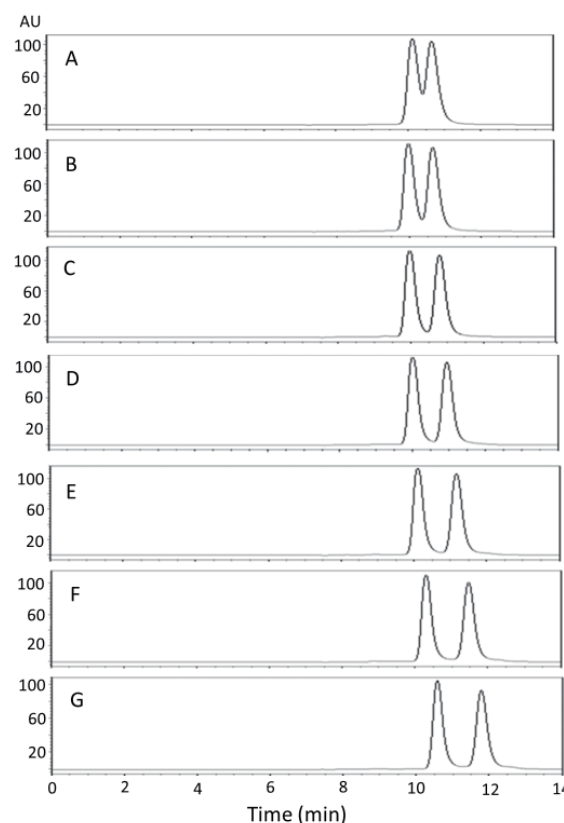


**Figure 2. Typical HPLC chromatograms of enantiomeric resolution of eriodictyol on Chiral Amylose-C column.** Mobile phase: (A) 2-propanol; (B) *n*-hexane-2-propanol, 5:95 (v/v); (C) *n*-hexane-2-propanol, 10:90 (v/v); (D) *n*-hexane-2-propanol, 15:85 (v/v); (E) *n*-hexane-2-propanol, 20:80 (v/v); (F) *n*-hexane-2-propanol, 25:75 (v/v); (G) *n*-hexane-2-propanol, 30:70 (v/v), at 0.5 mL/min in all cases.

by the positive and negative CD signals at 284 nm, the *R*-enantiomer eluted as the first peak (Figure 3). Beside to obtain CD signal at a chosen  $\lambda$ , the complete CD spectrum of the eluting peak could also be obtained in a stop-flow mode. Based on the obtained CD spectra, the absolute configuration of the elutes could also be determined.

### 3.2. Effects of racemic and enantiomeric eriodictyol on $H_2O_2$ -induced cytotoxicity in EA.hy926 cells

To evaluate the efficacy of racemic and enantiomeric eriodictyol on  $H_2O_2$ -induced cytotoxicity, EA.hy926 cell line was used. Firstly, cells were treated with 200  $\mu M$   $H_2O_2$  in the presence or absence of racemic and enantiomeric eriodictyol (5, 10, 15, 20  $\mu M$ ), and the cell viability was assessed by performing MTT assay. All the compounds tested were clearly able to block the cytotoxic effects of  $H_2O_2$  on EA.hy926 cells, and also both enantiomers and the corresponding racemate were almost equipotent (Figure 4A).

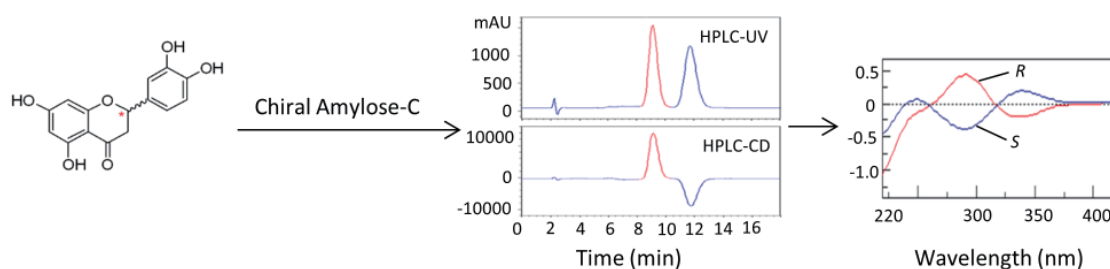


**Figure 3.** HPLC-CD chromatograms and CD spectra of the eluted peaks of eriodictyol on Chiral Amylose-C. Mobile phase: *n*-hexane-2-propanol, 25:75 (v/v).

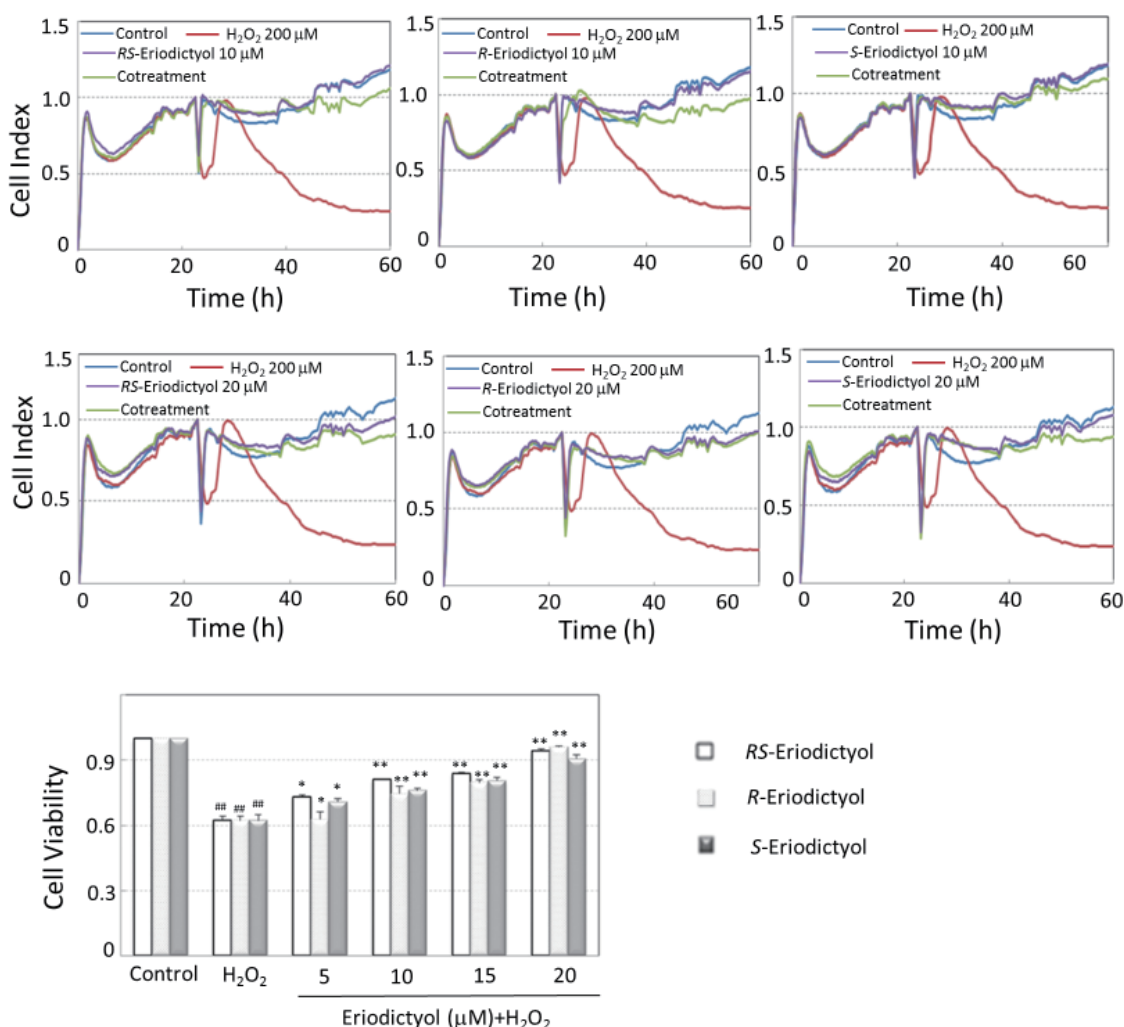


**Figure 4.** Protective effects of *RS*-, *R*- and *S*-eriodictyol on  $H_2O_2$ -induced EA.hy926 cell injury. (A) EA.hy926 cells were treated with 200  $\mu M$   $H_2O_2$  alone or co-treated with indicated concentrations of *RS*-, *R*- and *S*-eriodictyol for 24 h, and cell viability was determined by MTT assay. Data are presented as mean  $\pm$  SD of three independent experiments.  $^{\#} p < 0.01$  versus untreated cells and  $^* p < 0.05$ ,  $^{**} p < 0.01$  versus  $H_2O_2$ -treated cells. (B) EA.hy926 cells were treated with 200  $\mu M$   $H_2O_2$  alone or co-treated with indicated concentrations of *RS*-, *R*- and *S*-eriodictyol, and cell viability was determined by the xCELLigence live cell analysis system.

The xCELLigence live cell analysis system can be used as a rapid monitoring tool for cellular viability and be applied in toxicity testing of xenobiotics using *in vitro* cell cultures. For the assay of the protective effects of racemic and enantiomeric eriodictyol against H<sub>2</sub>O<sub>2</sub>-induced cytotoxicity, the xCELLigence live cell analysis system was used as the second testing method. After seeding the EA.hy926 cells to E-plates, the proliferation, attachment and spreading of the cells was monitored every 15 min by the xCELLigence system. Approximately 24 h after seeding, the cells were treated with DMSO, H<sub>2</sub>O<sub>2</sub>, racemic/enantiomeric eriodictyol, or in combination, and cell growth was monitored for a period of up to 48 h. H<sub>2</sub>O<sub>2</sub> (200 μM) could elicit significant cytotoxicity in EA.hy926 cells, which displayed as sharp CI decreasing, whereas treatment with racemic/enantiomeric eriodictyol (10 and 20 μM) alone did not affect the cell growth. However cotreatment significantly improved cell

survival as judged by slight CI decreasing compared with H<sub>2</sub>O<sub>2</sub> treatment alone (Figure 4B). Consistent with the results tested by MTT assay, both enantiomers and the corresponding racemate of eriodictyol were equipotent.

### 3.3. Effects of enantiomeric eriodictyol on DNA condensation and H<sub>2</sub>O<sub>2</sub>-induced apoptosis in EA.hy926 cells

DAPI staining revealed that nuclear DNA condensation and nuclear fragmentation occurred after treatment with 200 μM H<sub>2</sub>O<sub>2</sub> for 24 h. Pretreatment with both *R*- and *S*-eriodictyol inhibited these apoptotic features (Figure 5). Annexin V cell surface staining followed by flow cytometry analysis also showed similar results. After exposure to 200 μM H<sub>2</sub>O<sub>2</sub> for 24 h, the apoptotic rate of cells increased from 8.95 ± 0.2% to 33.59 ± 2.0%. Pretreatment with both racemic and enantiomeric

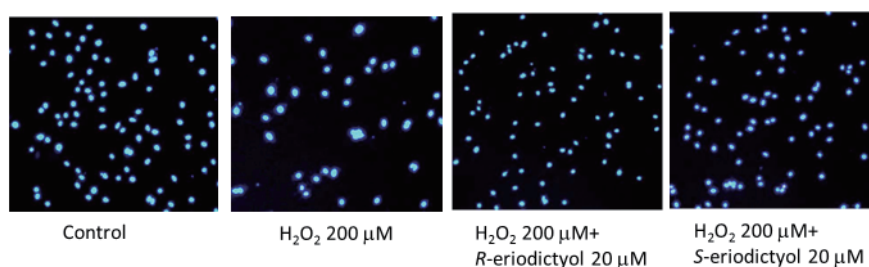


Figure 5. DAPI staining of nuclei and assessment of nuclear morphology.

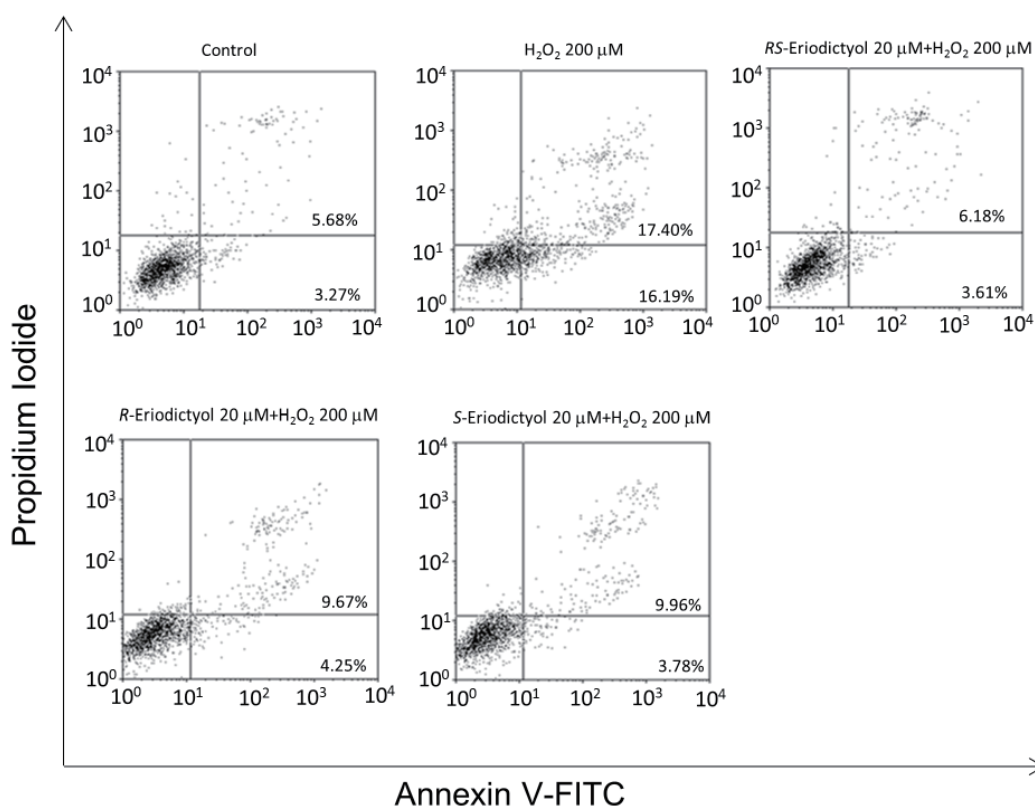
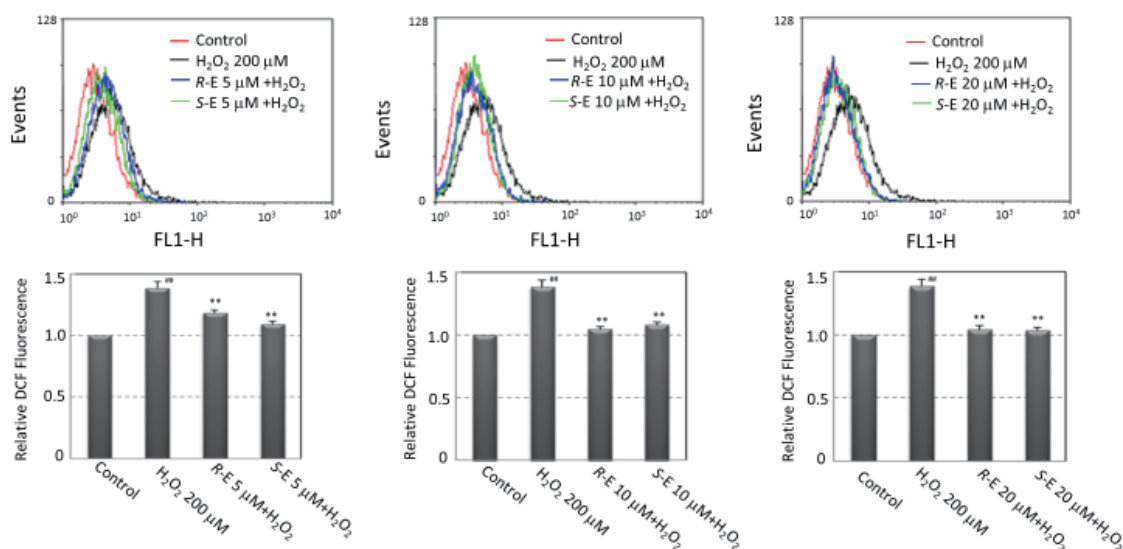


Figure 6. Cellular apoptosis was assayed by annexin V-FITC and PI staining, and analyzed with flow cytometry. Quantification of apoptotic cells are from three independent experiments. Values are expressed as mean ± SD.



**Figure 7.** Effects of *R*- and *S*-eriodictyol on  $\text{H}_2\text{O}_2$ -induced intracellular ROS level in EA.hy926 cells. The original flow cytometry results are shown in upper panel. The relative fluorescence intensity shown in lower panel are presented as mean  $\pm$  SD of three independent experiments. <sup>#</sup> $p < 0.01$  versus untreated cells and <sup>\*\*</sup> $p < 0.01$  versus  $\text{H}_2\text{O}_2$ -treated cells.

eriodictyol (20  $\mu\text{M}$ ) reduced the rate of apoptosis. These results indicated that *R*- and *S*-eriodictyol have anti-apoptotic effects against  $\text{H}_2\text{O}_2$ -induced apoptosis in EA.hy926 cells, and the anti-apoptotic effects were almost the same for the two enantiomers (Figure 6).

### 3.4. Effects of enantiomeric eriodictyol on intracellular ROS production

To determine the effects of compounds on ROS induction, DCFH-DA and flow cytometry were used to detect intracellular peroxide levels. As shown in Figure 7, when EA.hy926 cells were exposed to 200  $\mu\text{M}$   $\text{H}_2\text{O}_2$  for 24 h, the intracellular ROS levels increased significantly compared with untreated cells. Treatment with both *R*- and *S*-eriodictyol attenuated the increase of ROS induced by  $\text{H}_2\text{O}_2$  in a dose-dependent manner, and the inhibiting intracellular ROS effects were almost the same for the two enantiomers.

## 4. Conclusion

Oxidative stress is an imbalance between the production of ROS and antioxidant defense mechanisms, potentially leading to cellular damage. Oxidative stress has a key role in the development of cardiovascular and/or cerebrovascular diseases. This phenomenon is mainly mediated by an enhanced ROS production by the vascular endothelium with its consequent dysfunction. Eriodictyol was chosen as an antioxidant as increasing evidences indicates the protection activity of the compound in many kinds of cellular disorders characterized by ROS overproduction (1, 7). Although there are a certain number of investigations detailing the antioxidant activity of the racemic eriodictyol (1, 4, 5, 7), no studies have properly assessed the differences

in activity between the enantiomers of eriodictyol. This work reports for the first time the comparison of effects of *R*- and *S*-eriodictyol against  $\text{H}_2\text{O}_2$ -induced oxidative stress in EA.hy926 cells. The results showed that eriodictyol could be resolved well on Chiral Amylose-C column. The two enantiomers of eriodictyol appeared to be almost equally effective in inhibiting  $\text{H}_2\text{O}_2$ -induced cell viability reduction and cell apoptosis, and also equipotent in decreasing intracellular ROS levels.

## Acknowledgments

Financial support of the National Natural Science Foundation (No. 81173528) and (No. Y2007C038) are gratefully acknowledged.

## References

- Rossato MF, Trevisan G, Walker CI, Klafke JZ, de Oliveira AP, Villarinho JG, Zanon RB, Royes LF, Athayde ML, Gomez MV, Ferreira J. Eriodictyol: a flavonoid antagonist of the TRPV1 receptor with antioxidant activity. *Biochem Pharmacol.* 2011; 81:544-551.
- Lee E, Jeong KW, Shin A, Jin B, Jnawali HN, Jun BH, Lee JY, Heo YS, Kim Y. Binding model for eriodictyol to Jun-N terminal kinase and its anti-inflammatory signaling pathway. *BMB Rep.* 2013; 46:594-599.
- Mandalari G, Bennett RN, Bisignano G, Trombetta D, Saija A, Faulds CB, Gasson MJ, Narbad A. Antimicrobial activity of flavonoids extracted from bergamot (*Citrus bergamia* Risso) peel, a byproduct of the essential oil industry. *J Appl Microbiol.* 2007; 103:2056-2064.
- Le, ER, Kim JH, Choi HY, Jeon K, Cho SG. Cytoprotective effect of eriodictyol in UV-irradiated keratinocytes via phosphatase-dependent modulation of both the p38 MAPK and Akt signaling pathways. *Cell Physiol Biochem.* 2011; 27:513-524.
- Johnson J, Maher P, Hanneken A. The flavonoid,

- eriodictyol, induces long-term protection in ARPE-19 cells through its effects on Nrf2 activation and phase 2 gene expression. *Invest Ophthalmol Vis Sci.* 2009; 50:2398-2406.
6. Lou H, Jing X, Ren D, Wei X, Zhang X. Eriodictyol protects against H<sub>2</sub>O<sub>2</sub>-induced neuron-like PC12 cell death through activation of Nrf2/ARE signaling pathway. *Neurochem Int.* 2012; 61:251-257.
  7. Zhang WY, Lee JJ, Kim Y, Kim IS, Han JH, Lee, SG, Ahn MJ, Jung SH, Myung CS. Effect of eriodictyol on glucose uptake and insulin resistance in vitro. *J Agric Food Chem.* 2012; 60:7652-7658.
  8. Bucolo C, Leggio GM, Drago F, Salomone S. Eriodictyol prevents early retinal and plasma abnormalities in streptozotocin-induced diabetic rats. *Biochem Pharmacol.* 2012; 84:88-92.
  9. Brocks DR. Drug disposition in three dimensions: an update on stereoselectivity in pharmacokinetics. *Biopharm Drug Dispos.* 2006; 27:387-406.
  10. Ito T, Ando H, Suzuki T, Ogura T, Hotta K, Imamura Y, Yamaguchi Y, Handa H. Identification of a primary target of thalidomide teratogenicity. *Science.* 2010; 327:1345-1350.
  11. Tomassoni D, Amenta F, Amantini C, Farfariello V, Mannelli LDC, Nwankwo IE, Marini C, Tayebati Sk. Brain activity of thioctic acid enantiomers: in vitro and in vivo studies in an animal model of cerebrovascular injury. *Int. J. Mol. Si.* 2013; 14:4580-4595.
  12. Gaggeri R, Rossi D, Daglia M, Leoni F, Avanzini MA, Manellic M, Juza M, Collina S. An eco-friendly enantioselective access to (R)-naringenin as inhibitor of proinflammatory cytokine release. *Chem. Biodivers.* 2013; 10:1531-1538.
  13. Yanez JA, Remsberg CM, Miranda ND, Vega-Villa KR, Andrews PK, Davies NM. Pharmacokinetics of selected chiral flavonoids: hesperetin, naringenin and eriodictyol in rats and their content in fruit juices. *Biopharm. Drug Dispos.* 2008; 29:63-82.
  14. Jeon Y, Kwon C, Cho E, Jung S. Carboxymethylated cyclophosphorase as a novel chiral additive for the stereoisomeric separation of some flavonoids by capillary electrophoresis. *Carbohydr Res.* 2010; 345:2408-2412.
  15. Asztemborska M, Miskiewicz M, Sybilska D. Separation of some chiral flavanones by micellar electrokinetic chromatography. *Electrophoresis.* 2003; 24:2527-2531.
  16. Caccamese S, Caruso C, Parrinello N, Savarino A. High-performance liquid chromatographic separation and chiroptical properties of the enantiomers of naringenin and other flavanones. *J Chromatogr A.* 2005; 1076:155-162.
  17. Guo X, Li C, Duan L, Zhao L, Lou H, Ren D. Separation of the enantiomers of naringenin and eriodictyol by amylose-based chiral reversed-phase high-performance liquid chromatography. *Drug Discov Ther.* 2012; 6:321-326.
  18. Ren D, Yuan J. Studies on the chemical constituents of *Dracocephalum rupestre*. *Zhong Cao Yao.* 1997; 28:74-76.
  19. Wang XJ, Sun Z, Chen W, Eblin KE, Gandolfi JA, Zhang DD. Nrf2 protects human bladder urothelial cells from arsenite and monomethylarsonous acid toxicity. *Toxicol Appl Pharmacol.* 2007; 225:206-213.
  20. Hu Q, Zhang DD, Wang L, Lou H, Ren D. Eriodictyol-7-O-glucoside, a novel Nrf2 activator, confers protection against cisplatin-induced toxicity. *Food Chem Toxicol.* 2012; 50:1927-1932.
  21. Urcan E, Haertel U, Styllou M, Hickel R, Scherthan H, Reichl FX. Real-time xCELLigence impedance analysis of the cytotoxicity of dental composite components on human gingival fibroblasts. *Dent Mater.* 2010; 26:51-58.
  22. Jiang T, Huang Z, Lin Y, Zhang Z, Fang D, Zhang DD. The protective role of Nrf2 in streptozotocin-induced diabetic nephropathy. *Diabetes.* 2010; 59:850-860.
- (Received September 15, 2014; Revised September 26, 2014; Re-revised October 23, 2014; Accepted October 24, 2014)